DISTRIBUTION STATEMENT A. Approved for public release; distribution is unlimited.

Aircraft Observations for Improved Physical Parameterization for Seasonal Prediction

Qing Wang
Meteorology Department, Naval Postgraduate School
Monterey, CA 93943
Phone: (831) 656-7716, Fax: (831) 656-3061 email: qwang@nps.edu

Award # N0001414WX20352

LONG-TERM GOAL

The long-term goal of this project is to improve the representation of fractional low-level clouds in the medium-range forecast models.

OBJECTIVES

The objectives of the NPS project is to understand the physical processes involved in boundary layers covered by fractional cloudiness and to make extensive measurements to address critical issues in cloud and turbulence parameterizations for improvements of extended forecasts.

APPROACH

The general approach of NPS research in this project is to understand the physical processes in stratocumulus-topped boundary layers through extensive data analyses of measurements from boundary layers with various macrophysics properties of stratocumulus clouds. Satellite data are used in conjunction with the aircraft measurements. The field campaign using the CIRPAS Twin Otter, which occurred in August/September 2012, will be referred to as Unified Physical Parameterization for Extended Forecast 2012 field project (UPPEF2012).

Qing Wang is responsible for the overall project. In FY14, analyses of the UPPEF measurements were aided by Lt. Kyle Franklin as part of his thesis research. NRC postdoc, Dr. Denny Alappattu, were also involved in the data analyses of UPPEF2012.

WORK COMPLETED

Our work in FY14 focused on aircraft data analyses on the scales and physical processes in small scale cloud breaks. Satellite measurements of the cloud irradiance are used to air the analyses. Specific work done includes:

1. Analysis of satellite imagery of horizontally extensive coastal stratocumulus layers with closed cell mesoscale cellular convection (MCC) near the coast transitioning to open cell MCC further offshore.

2. Analyses of aircraft in situ measurements trough the cloud layers focusing on the characteristics of the narrow downdrafts that resulted in the apparent cloud breaks seen on the satellite imagery.

RESULTS

Mesoscale cloud structure from Satellite: Figure 1a shows an example of the satellite cloud imagery indicating the variability in cloud scales in the near-shore and offshore regions on UPPEF RF05 at the time of Twin Otter measurements. During this research flight, the stratocumulus-topped boundary layer (STBL) transitions from near-shore closed cell MCC to offshore open cell MCC. The spectral characteristics of these two distinct regions are analyzed. Figure 1a shows the near-shore transects in the closed cell MCC region in which the research flight was conducted. Further offshore, open cell MCC becomes prominent, and synoptic winds veer slightly, hence the adjustment to the orientation of the offshore transects.

Figure 1b shows that the spectra characteristics calculated from the individual transect match well within each region, this is a verification of the spectral uniformity within each region. The area averaged power spectral density (PSD) calculated from these transects, shown in Figure 1c, indicate an offshore peak of .087 m^{-1} in wavenumber and a broad peak between .105 and .182 m^{-1} wavenumbers in the near-shore region. The PSD for the two regions have the same general shape. However, the PSD of the offshore region is two orders of magnitude larger than the near-shore region across the .03 to .20 m^{-1} wavenumber range and one order of magnitude larger across the remaining wavenumbers. These peak wavenumbers correspond to offshore peak at 11.5 km, and near-shore peaks occur at 7 km and 9.5 km. The increase of cloud patches offshore is clearly seen in the satellite imageries. Similar analyses for another flight (RF10) show similar offshore evolution of the cloud structure with the offshore peak wavelength at 20 km and 8.5 km for the near-shore region (not shown). Further analyses of the imageries at different time of the day indicate that the PSDs appear to shift to larger wavelengths through the morning, particularly in the near-shore closed cell region. The early morning PSDs also shows more prominent peak energy compared to the late morning imageries. This suggests that convective motions, and hence cellular appearance, are more "organized" in the early morning (not shown).

Cloud breaks and downdrafts from aircraft measurements: Figure 2 shows an example of the spatial variability of key thermodynamics variables through the cloud layer. The key thermodynamic variables are in good agreement in the identifiable the convective downdrafts, with liquid water content (q_l), water vapor (q), and potential temperature (θ) all decreasing simultaneously. This is an indication of slightly dryer and colder air, resulting from the incorporation of dry air from above the boundary layer inversion into convective downdrafts, and subsequent evaporative and infrared cooling, resulting in denser and negatively buoyant air.

A spectral analysis was performed on vertical velocity, potential temperature, and cloud liquid water (Figure 3). In this example of an in-cloud leg (RF05, LL1 at ~500 m above surface), the spectral analysis of all three variables shows a clear PSD spike at the 8.2 km length scale. Similar analyses from other two similar legs of the same flight show peaks at the 8.2 and 10 km ranges. The length scale of maximum PSD corresponds closely with the findings from the satellite irradiance analyses.

Conditional sampling and statistical analyses of cloud breaks: A conditional sampling method is used to identify the cloud break downdrafts seen in the in-cloud in situ measurements. Figure 4a shows

that the identified events (indicated by the green gate function) appear to occur with a preferred spacing between events and a preferred width of event. To determine the magnitudes of these scales statistically, the probability density functions (PDF) were calculated for the respective quantities for two measurement legs of RF05 (Figures 4b and 4c). We found from this flight, that the distance between adjacent events is almost always less than five km, and is most often less than one km. This distance represents the spacing between cloud breaks. The PDF for the width of the cloud breaks indicates a peak between 50 and 100 meters, and all of the events were less than 300 meters wide. These statistical spatial characteristics indicate that these events occur at preferred length scales. The event spacing length scale is likely responsible for the secondary PSD spike observed at the one to two km length scale. This result indicates the existence of two discreet scales of variation within the closed cell MCC: turbulent scale cloud breaks imbedded within mesoscale circulations.

The relationship between dynamic and thermodynamic variable perturbations within the identified downdraft events are shown in Figures 35. The correlation between dynamic and thermodynamic properties within events is linearly correlated, which is more apparent between water vapor, potential temperature and vertical velocity. The corresponding correlation coefficients are given in Table 2, which show that the correlation coefficients are mostly positive, and between .1 and .7. This is an indication of a typically cooler and drier air within downdraft regions. Table 2 also shows a strong reduction in the magnitude of variable perturbations lower in the cloud level (LL8), this is an indication of the cloud breaks mixing with the environment further away from the cloud top.

IMPACT/APPLICATIONS

Analyses of UPPEF2012 data provide the basis of case selection for ongoing UPPEF modeling efforts. The new measurements by the CIRPAS Twin Otter under this project have proved to be a valuable dataset to further our understanding of physical processes affecting fractional clouds and therefore for obtaining improved parameterization in fractional cloud condition in forecast models.

RELATED PROJECTS

Related project is the ONR DRI on Unified Physical Parameterization for Extended Forecast.

PUBLICATIONS

Franklin, Kyle B. 2014: Mesoscale variability in coastal stratocumulus clouds Observed during UPPEF 2012, MS. Thesis, Naval Postgraduate School, March 2013.

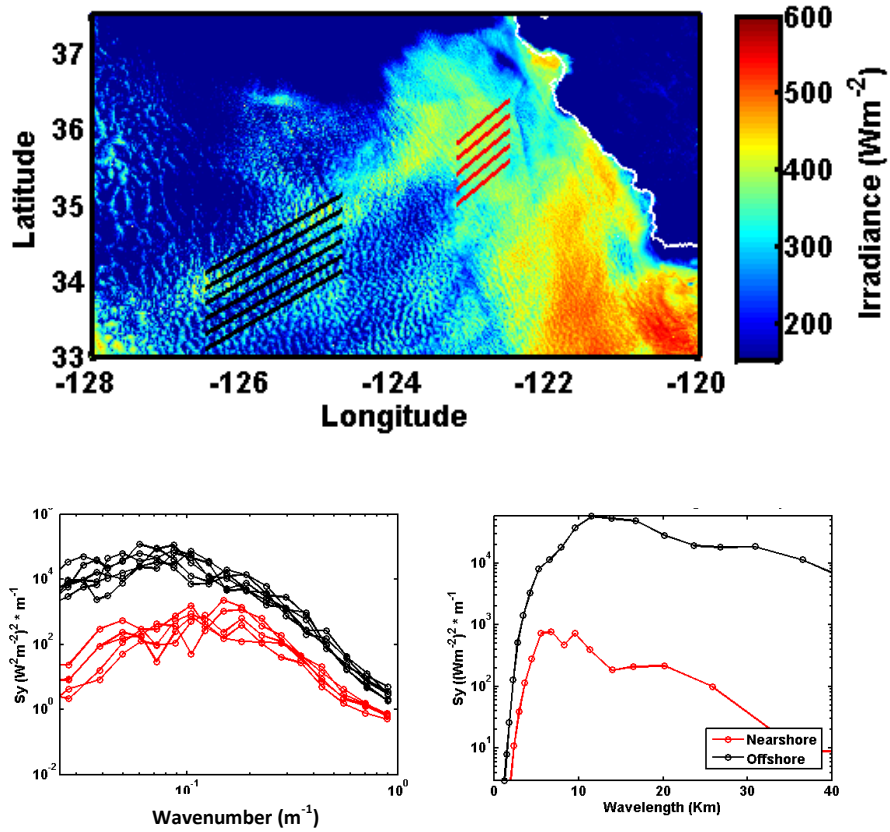

Figure 1. (a)Near-shore and offshore cross section locations at 1800 GM, (b) power spectra of irradiance for each selected near-shore (red)and offshore (black) 'legs' shown in (a), and (c) averaged power spectra corresponding from those shown in (b).

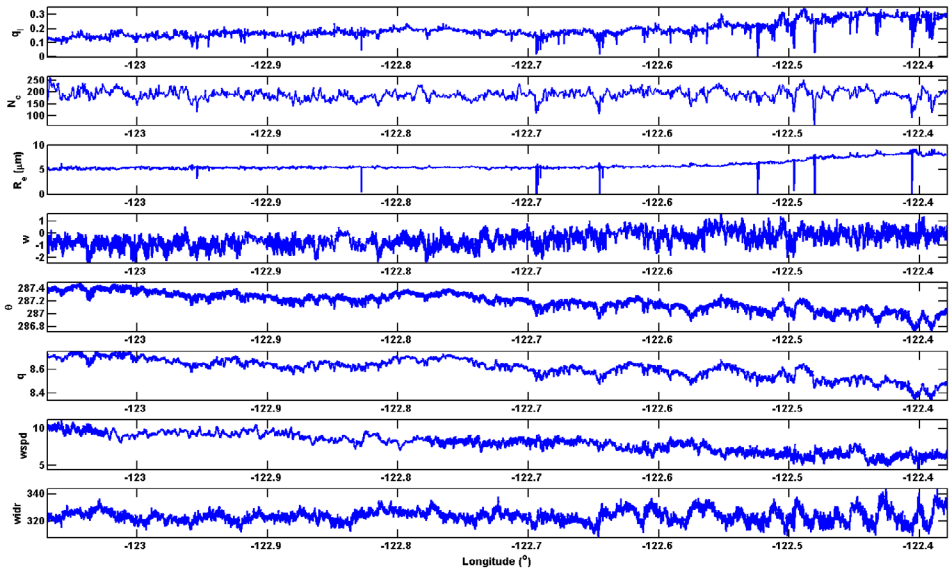

Figure 2. Spatial variations along the flight track observed from RF05 LL1. Shown here are cloud liquid water content (q_l), droplet number concentration (N_c) and droplet mean effective radius (R_e), vertical velocity (w), potential temperature (θ), water vapor (q), wind speed (wspd) and wind direction (wdir).

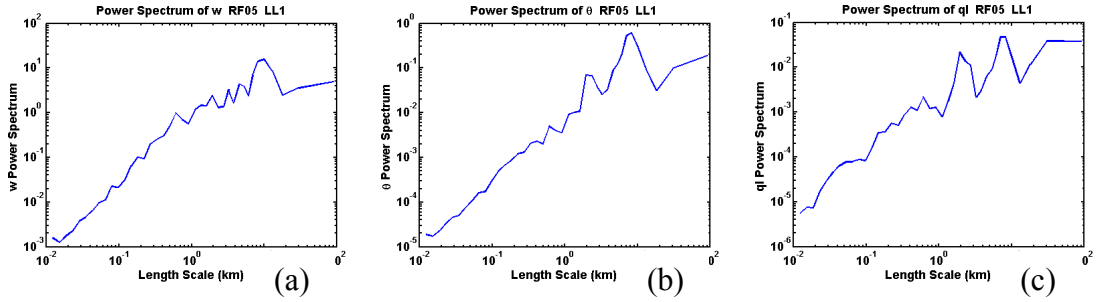

Figure 3. PSD for (a) vertical velocity, (b) θ, and (c) q_l for an in-cloud leg (LL1) on RF05 of UPPEF.

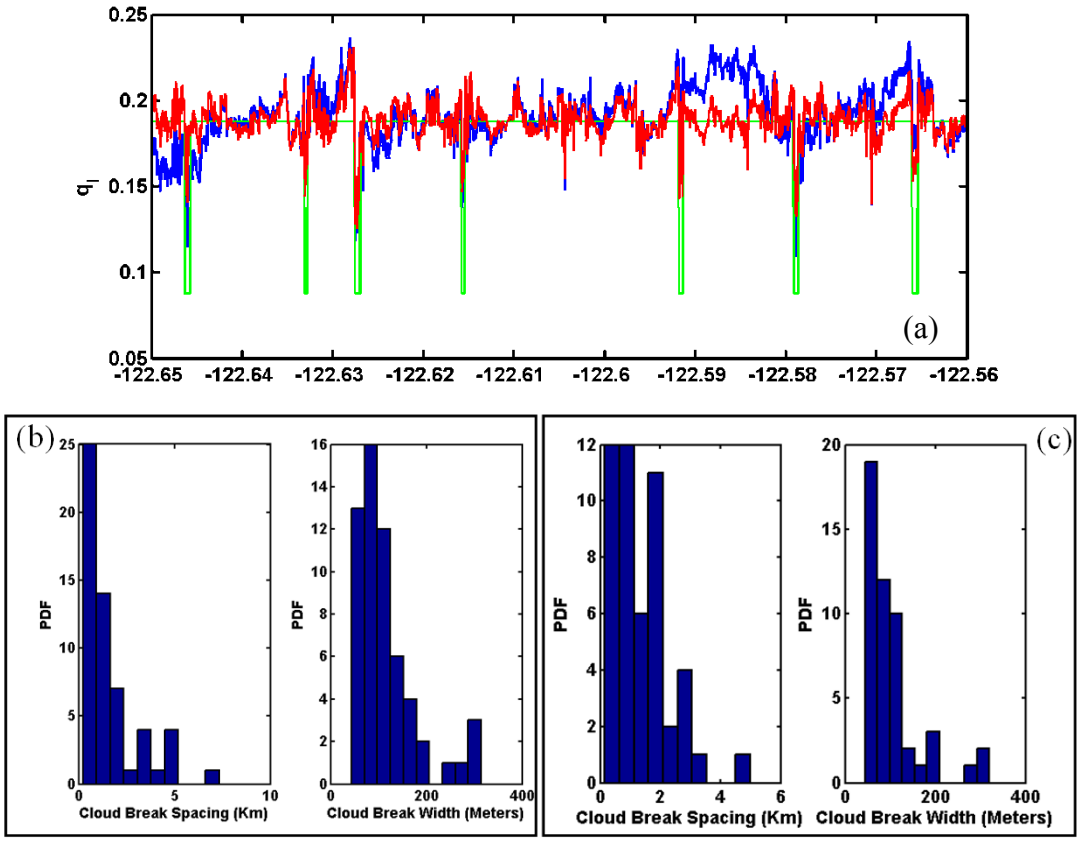

Figure 4. (a) Example of cloud break "events" indicated by a green gate function. The original liquid water content is shown in blue, high-pass filtered q_l is shown in red, (b) Event spatial characteristic PDFs for RF05 LL1, and (c) Same as in (b), except for LL3.

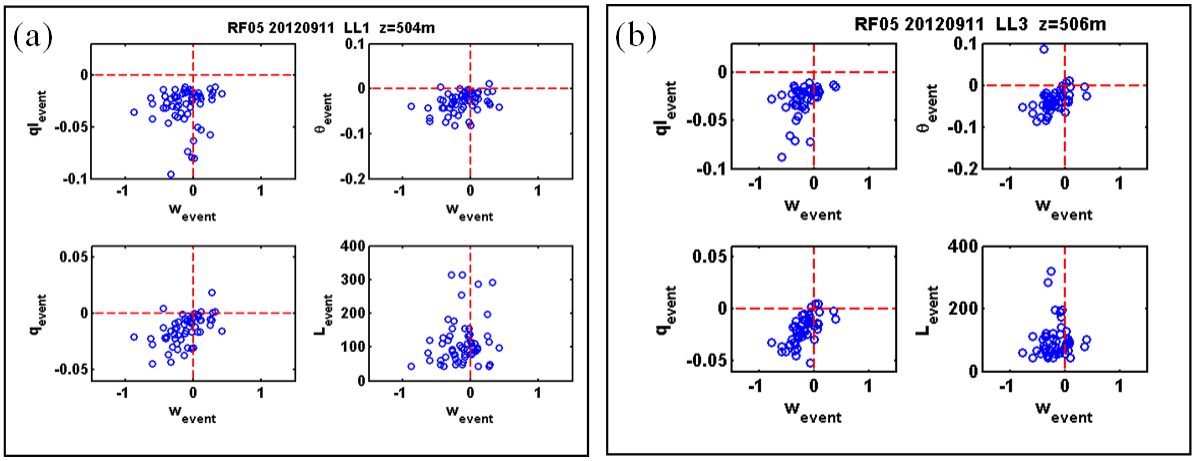

Figure 5. Correlation of event properties with event mean vertical velocity for RF05 (a) LL1 and (b) LL3. Although at the same levels, LL3 is further away from the local cloud top because of the higher cloud top at the LL3 location.

Table 1. Correlation coefficients between event averaged vertical velocity and water vapor, θ, and liquid water and event mean perturbations from each leg of RF05.

	R_{wq}	$R_{w\theta}$	R_{wql}	w_{event}	θ_{event}	q_{event}	q_{levent}
LL1	.5243	.3450	.0816	-.2499	-.0322	-.017	-.030
LL3	.0703	.0957	.2324	-.2745	-.0114	-.043	-.036
LL8	.6731	.2729	-.0450	-.1323	-.006	-.007	-.007